Impact Mechanism and Improvement Strategy on Urban Ventilation, Urban Heat Island and Urban Pollution Island: A Case Study in Xiangyang, China

著者	Zhan Qingming, Gao Sihang, Xiao Yinghui, Yang Chen, Wu Yihan, Fan Zhiyu, Wu Jiaqi, Zhan Meng
journal or publication title	International Review for Spatial Planning and Sustainable Development
volume	8
number	3
page range	68-86
year	2020-07-15
URL	http://doi.org/10.24517/00062358

doi: 10.14246/irspsd.8.3_68

International review for spatial planning and sustainable development, Vol.8 No.3 (2020), 68-86
ISSN: 2187-3666 (online)
DOI: http://dx.doi.org/10.14246/irspsd.8.3_68

Impact Mechanism and Improvement Strategy on Urban Ventilation, Urban Heat Island and Urban Pollution Island: A Case Study in Xiangyang, China

Qingming Zhan[1,2]*, Sihang Gao[1,2],Yinghui Xiao[1,2], Chen Yang[1,2], Yihan Wu[1,2], Zhiyu Fan[1,2],Jiaqi Wu[1,2],Meng Zhan[1,2]
1 School of Urban Design, Wuhan University
2 Collaborative Innovation Center of Geospatial Technology
** Corresponding Author, Email: qmzhan@whu.edu.cn*

Received: November 11,2019 Accepted: June 01, 2020

Key words: Urban Ventilation Corridors Planning, Urban Thermal Environment, Computational Fluid Dynamics, Geographically Weighted Regression, Remote Sensing, Urban Air Pollution

Abstract: There has been a growing interest in finding mitigation measures for urban heat islands and urban pollution islands that focus mainly on urban landscape mechanisms. However, relatively little research has considered spatial non-stationarity and temporal non-stationarity, which are both intrinsic properties of the environmental system, simultaneously. At the same time, the relevance of and differences between the thermal environment and air pollution has also been rarely discussed, and both issues are of great importance to urban planning. In this study, which is aimed at improving urban ventilation to reduce the urban heat island and urban pollution island effects, an urban ventilation potential evaluation, land surface temperature time-series clustering and air pollution source identification are comprehensively applied to identify the operational areas, compensation areas and ventilation corridors in Xiangyang, China, thus bridging the gap between academic research and urban planning. The specific research areas include: (1) defining the operational areas for urban ventilation corridor planning through an urban ventilation potential evaluation featuring urban morphology indicators, land surface temperature time-series clustering with *k*-means and an urban air pollution source diffusion analysis via the Hybrid Single-Particle Lagrangian Integrated Trajectory (HYSPLIT) and geographically weighted regression (GWR) methods; (2) identifying urban cold islands through land surface temperatures and delimiting the compensation areas in urban ventilation corridor planning; (3) designating urban ventilation corridors through an urban ventilation potential evaluation and computational fluid dynamics (CFD); and (4) improving urban ventilation corridor planning through defining operational areas, compensation areas and ventilation corridors as well as proposing corresponding control measures.

1. INTRODUCTION

Rapid urbanization has been changing urban forms and functions continuously (Stone, 2009), as manifested in increasing surface roughness (Chen, Liang & Dirmeyer, 2019), decreasing ventilation potential, the expansion of impervious surfaces (Yang, Chen et al., 2019) and the weakening of surface transpiration (Dienst, Lindén, & Esper, 2018). These changes make

it difficult to effectively evaluate the energy dissipation and waste emissions generated by populations and industries over short periods of time (Kuang et al., 2015). Furthermore, interactions between humans and the environment aggravate a variety of urban problems, such as urban heat islands and urban pollution islands, and exert a dramatic impact on human health and well-being as well as potentially increasing cause-specific morbidity and mortality (Patz et al., 2005). It has been repeatedly proven that urban morphology, urban landscape composition and urban landscape configuration have significant effects on urban ventilation, the urban thermal environment and urban near-surface aerosol properties (Song et al., 2014; Wang, Z.-b. & Fang, 2016; Wang, J., Zhan, & Guo, 2016; Peng et al., 2018). Hence, the detailed spatial patterns of these different indicators, for which the most widely used model is the local climate zone (LCZ) model put forward by Oke in 2012, are sought by urban planners (Shi et al., 2019). However, the spatial variations in the intra-city air pollution and thermal environment have rarely been quantified simultaneously. Due to the differences between the surface thermal environment and air pollution in terms of operational scale and affecting factors, further discussion is necessary in order to extend the LCZ model for the control of an urban pollution island (Chen, Lei et al., 2018). Therefore, we seek to provide a rough framework that can roughly partition a control area while limiting detailed information to avoid being misleading. Urban ventilation corridor planning, which originated in Germany, is used to divide an urban area's underlying surface into three basic planning control zones: the operational areas (where thermal pollution and air pollution exist), compensation areas (the areas bringing in fresh air) and ventilation corridors (strips with low roughness linking the operational and compensation areas). Hence, in order to reduce the urban heat island and urban pollution island effects in Xiangyang, China, this study aims to investigate the city's urban ventilation through an urban ventilation potential evaluation, land surface temperature (LST) time-series clustering and air pollution source identification. The results will then be applied comprehensively to divide the city into operational areas, compensation areas and ventilation corridors, thus bridging the gap between academic research and urban planning.

Urban ventilation research is divided into two parts at the intra-city scale, namely, urban ventilation simulation, which is accomplished via a weather forecast model and computational fluid dynamics (CFD) model (Kadaverugu et al., 2019), and conducting ventilation potential evaluations via urban morphological indicators, which can be used specifically for urban planning (Javanroodi, Mahdavinejad, & Nik, 2018). Meteorological simulation models and weather forecasting models are generally adopted in urban ventilation simulation and predictions done at large regional scales and include the Weather Research and Forecast (WRF) model (Sharma et al., 2016) and Mesoscale Meteorological model (known as the MM5 model) (Gsella et al., 2014), both of which are non-hydrostatic models. The MM5 model is designed to simulate atmospheric circulation at the regional and megalopolis scales. The WRF model is mainly applied to monitor, simulate and predict the real-time meteorological conditions at an intra-city scale (~10m-~10km), and the most suitable grid unit for simulation is 1km*1km (Yang, B., Zhang, & Qian, 2012). In terms of urban climatological studies, the WRF model is not only a good predictive method but also a good retrospective method for obtaining continuous, smooth wind fields at a regional scale from the past. Compared with the traditional method of obtaining wind fields through ground stations, its main advantages are: (1) it is less influenced by the number of stations and can obtain a continuous, smooth regional wind field instead of the wind speeds

and directions from a few locations without the need to make up the smoothness; (2) the algorithm can correct the wind field at the current time according to the wind field conditions at a nearby time point, thus reducing local interference and obtaining a typical wind field distribution pattern. Therefore, the WRF model is also widely used in urban climate studies to describe typical wind environmental patterns at the urban and regional scales.

Translating knowledge of the interactions between physical forms and the climate into practical planning applications to address urban ventilation effectively has been a challenge. Therefore, it will be advantageous to find the widely discussed relationship between urban form and urban ventilation because it corresponds to urban design and planning directly. Climatologists have been studying how urban structures affect local microclimatic conditions. The local climate zone (LCZ) scheme, put forward by Stewart and Oke (Stewart & Oke, 2012), attaches urban morphology to urban climatic conditions through a set of parameters selected to define the LCZ class. These geometric parameters and land cover indicators include building indicators and terrain roughness. In an urban climatic study conducted by Xu et al. (2017) in Hong Kong, the relationship between architectural morphological indicators for urban ventilation and intra-urban land surface temperature was discovered, and the significant influence of surface roughness on wind speed over the city was also verified. The widely used urban morphology indexes include the building density (BD) (Sun et al., 2019), building height (BH) (Yin et al., 2018), building volume density (BVD) (Xu et al., 2017), sky view factor (SVF) (He, Ding, & Prasad, 2019) and fa çade area ratio (FAR) (Tsichritzis & Nikolopoulou, 2019). In terms of ventilation potential evaluations, it has been common practice to utilize morphology indicators for city-scale analyses.

Finding a suitable method for classifying urban areas dealing with urban climate problems has always been a challenge for urban planners from the perspectives of both the settlement mechanism and physical phenomena (Fu & Weng, 2016). The introduction of urban climate maps, which apply city subdivision ideas widely used in urban planning to urban climatology, bridges the gap between urban climate research and urban design, and facilitates the implementation of specific planning measures (Oke et al., 2017). However, models based on a single snapshot analysis are often limited due to the interference of chance factors, such as atmospheric hydrological conditions (Wang, C. et al., 2019). Time series clustering is a potential research paradigm that uses machine learning methods to group objects based on their spatio-temporal similarities and is widely used in the analysis of spatio-temporal data in geographic information science (Liu et al., 2018; Liu, Zhan, Yang, et al., 2019). It identifies potential patterns of change in climate elements through the identification of inter-group variances and trend lines within different regions based on multiple images, thereby effectively zoning the climate and reducing the interference in the smoothness caused by sensor errors and hydrological conditions.

Compared to the urban heat island research that is already quite common at the intra-urban scale, intra-urban air pollution research has encountered difficulties. Having benefited from an abundance of observation tools and the proliferation of monitoring sites, air pollution research at the traditional regional scale is increasingly being extended to the urban scale. Urban-scale air pollution research is primarily concerned with the impact of urban surface elements and human productive life on the formation and spread of pollutants. As in urban heat island studies, geographically weighted regression (GWR) is widely used in these studies to remove the effect of spatial heterogeneity (Xie, W., Deng, & Chong, 2019) on the fitting effect and capture the main factors

influencing the diffusion of generated air pollution in different geographical subdivisions (Wang, Z.-b. & Fang, 2016; Yang, C. et al., 2018). However, these findings suggest that traditional climate research frameworks may be limited for air pollution research, as pollutant concentration monitoring is often influenced by the diffusion of aerosol flows at larger regional scales, effectively limiting the significance of regression results at the urban scale. Hence, distinguishing between exogenous (Dimitriou & Kassomenos, 2014) and endogenous (Schindler, Caruso, & Picard, 2017) pollution to better interpret urban-scale regression results is an emerging need. The Hybrid Single-Particle Lagrangian Integrated Trajectory model (HYSPLIT), developed by the National Oceanic and Atmospheric Research Center (NOAA), provides a new method for determining the proportion of pollution sources based on the trajectory of aerosols and aerosol masses to better identify dominant gas sources in a city, thus allowing the different impacts of exogenous and endogenous pollution to be assessed more accurately. At the same time, differences in the influencing factors for air pollution and urban heat islands contribute to the variability between the two problems, with air pollution being more associated with human activity, while urban heat islands are more affected by impervious surfaces and vegetation. These variations affect operational area identification and highlight the need to consider both effects when delineating an operational area.

Based on the above background, this study will identify the characteristics of the urban surface microclimate and explore the main influencing factors from three perspectives, namely, urban ventilation, the urban thermal environment and urban air pollution. The purpose of this study is to: (1) define the operational areas for urban ventilation corridor planning through an urban ventilation potential evaluation using urban morphology indicators, land surface temperature time-series clustering with *k*-means and HYSPLIT and GWR urban air pollution source diffusion analyses; (2) identify urban cold islands through land surface temperatures and identify the compensation areas for urban ventilation corridor planning; (3) designate urban ventilation corridors through an urban ventilation potential evaluation and CFD; and (4) improve general urban ventilation corridor planning through identifying operational areas, compensation areas and ventilation corridors as well as proposing corresponding control measures.

2. DATASETS AND METHDOLOGY

2.1 Xiangyang, China

Using the urban ventilation study and planning done for Xiangyang as a case study, this paper analyses urban ventilation, urban thermal environment and urban air pollution problems through the technical routes mentioned above and puts forward urban planning suggestions to solve these problems. In recent years, Xiangyang, which is a medium-sized city in the Yangtze river basin, has suffered from an intensified urban heat island effect and an increasingly serious urban pollution problem due to rapid industry development and continuous expansion. By using Xiangyang as an example, on the one hand, the distribution rules for the urban heat island effect in medium-sized cities under subtropical monsoon climate conditions and the differences between the urban heat island effect in large cities and mega-cities can be explored. On the other hand, air pollution control strategies for cities

transformed by heavy industry in central China can also be explored. As shown in *Figure 1*, using Landsat 8 images collected on July 28, 2015, we selected a 30.5 km×20 km area for this study that covers the downtown area of Xiangyang and the industrial parks around the city. The research area also fully illustrates the heterogeneity of the land cover in terms of bodies of water, vegetation and the intensities of built-up areas. The upper left and lower right coordinates of the study area are 32 °09'24"N, 112 °04'18"E and 31 °52'46"N, 112 °16'43"E, respectively (as shown in *Figure 1*).

2.2 Data Sets

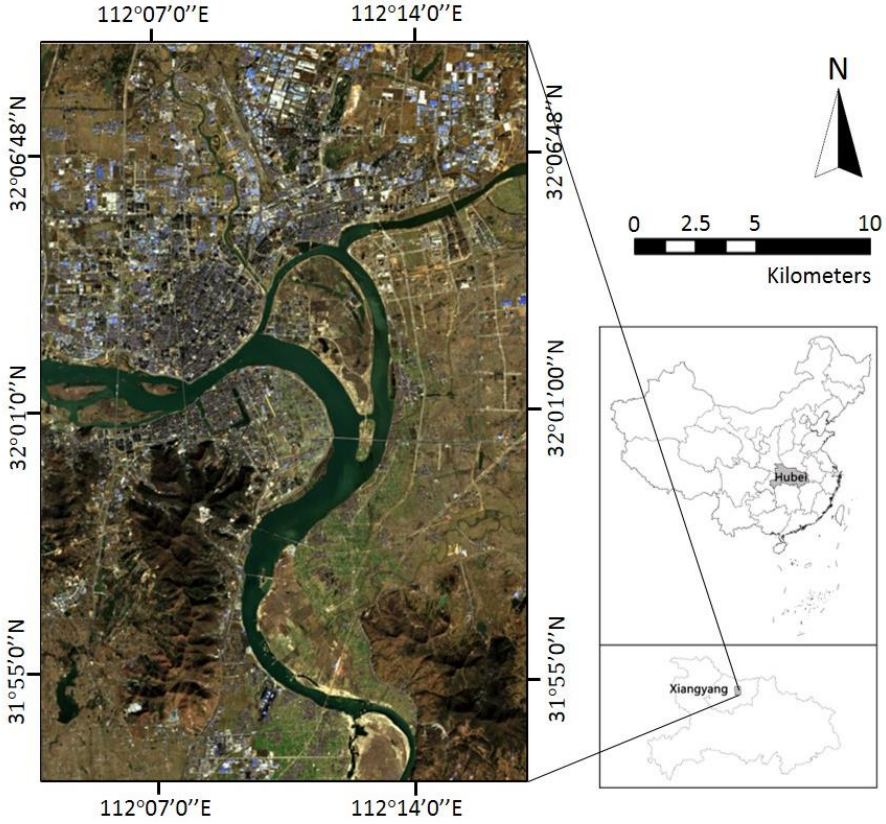

Figure 1. The study area represented by the Landsat 8 image acquired on 28 July 2015

2.2.1 Land Surface Temperature (LST)

In this paper, remote sensing images collected by the Landsat-8 Operational Land Imager (OLI) were used for surface temperature inversion at a spatial resolution of 30m. The classic radiative transfer equation (RTE) (Yu, Guo, & Wu, 2014) was employed to retrieve the LST from the selected Landsat 8 Thermal Infrared Sensor (TIRS) scenes. In order to study the long-term law of evolution for the surface thermal environment and make it possible to consider the smallest accidental errors made under different climatic and hydrological conditions, this study selected annual images from 2013 to 2016, that is, from August 7, 2013, July 9, 2014, July 28, 2015 and June 28, 2016. The images for all four years are from the summer; thus, they were taken under similar atmospheric and hydrological conditions, minimizing the effect of unexpected errors on the experimental results (*Table 1*).

Table 1. Data for the representative images from each year for all four years

Year	Image Data	Maximum Temperature (◦C)	Minimum Temperature (◦C)	Average Relative Humidity	Average Wind Force (km/h)
2013	7 Aug	38	29.3	51	14.4
2014	9 Jul	29.4	21.7	70	7.8
2015	28 Jul	34.2	26.7	67	15.9
2016	28 Jun	29.4	24.8	68	9.8

2.2.2 Urban Air Pollution

The air pollution data used in this paper comes from ground measurement stations. A total of 180 micro-stations for air pollution monitoring were set up in the downtown area, Yujiahu industrial park in the south and Xiangzhou industrial park in the north to monitor the PM2.5, PM10, SO_X, NO_X and O_3 contents. Particulate matter with an aerodynamic diameter of less than 2.5 μm (PM2.5) (Xie, Y. et al., 2015) has been recognized as one of the principal pollutants that degrades air quality and increases health burdens. In this paper, based on the PM2.5 data, the kriging interpolation method is adopted to obtain air pollution distribution images for the entire range. The kriging method is a regression algorithm used for spatial modelling and the prediction (interpolation) of random processes/random fields that is based on a covariance function (Gholizadeh et al., 2019). In certain random processes, such as inherently stationary processes, the kriging method can provide optimal linear unbiased estimates. The kriging method and its improved algorithm are widely used in the inversion and interpolation of air pollution data at monitoring points. For this paper, the monitoring data obtained on February 9, 2018 were selected to interpolate the air pollution distribution within the study area. The meteorological conditions on that day were good and not affected by exogenous pollution, so interference could be discounted in the study of endogenous pollution.

3. METHDOLOGY

As shown in *Figure 2*, the city will be partitioned by various methods to improve urban ventilation and cope with the urban heat island and pollution island effects. Specifically, we plan to identify the operational areas through GWR and HYSPLIT, identify the compensation areas through time series clustering, and identify the ventilation corridors through a WRF ventilation simulation and a ventilation potential evaluation.

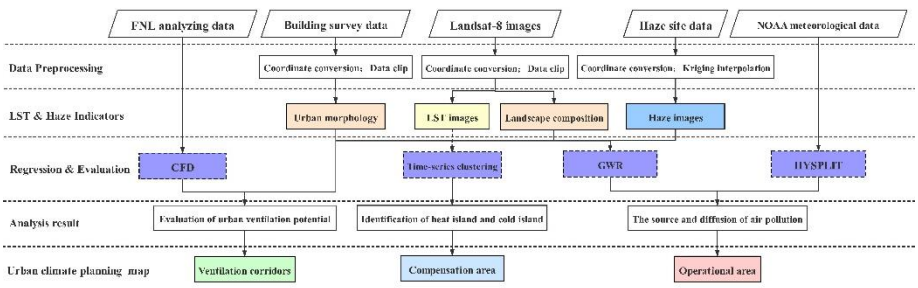

Figure 2. The methodological framework used in this study

3.1 Urban Ventilation Evaluation

3.1.1 Weather Research and Forecast (WRF) Model

The WRF model is the latest mesoscale model and is widely used in weather forecasting and climatology research. There are two operational models available: one is a real case model that simulates real cities, and the other is an ideal case model that simulates virtual cities (Zhou & Chen, 2018). The WRF model is a fully compressible non-hydrostatic model. The initial and boundary conditions of the model were developed by the National Centers for Environmental Prediction (National Centers for Environmental Prediction-Final, NCEP-FNL), which conducts a global analysis at a resolution of 1 °×1 °. The FNL analysis is done with data from the global data assimilation system (GDAS), which collects observations continuously from sources such as the global telecommunications system (GTS). The transverse boundary conditions of the model are updated every 6 hours, and the geophysical parameters, such as topography, land use, vegetation type, vegetation composition and soil type, are taken from the data set maintained by the United States Geological Survey (USGS). The model is configured using a triple-nested domain, in which the outer two domains (D1 and D2) use the default USGS Land-Use/Land-Cover (LULC) scheme and the innermost (3) domain is classified according to the new Landsat-based classification. The WRF model can predict the wind speed, wind direction, temperature, water vapor, cloud cover, precipitation and pressure distributions for different underlying surfaces. However, the basic WRF model does not fully consider human impacts and urban morphologies (Jiménez et al., 2010).

In this study, GDAS observation data are used to simulate the ventilation conditions of Xiangyang city in the winter and summer, respectively. The basic grid unit is set as 1km, and the simulation range is downtown Xiangyang and the Yujiahu industrial zone. The underlying surface condition is based on the Landsat land cover data for the system. The spatial distributions of the wind speed, wind direction and wind frequency are obtained by inversion.

3.1.2 Ventilation Potential Evaluation

According to related research, the average building height, building density, building volume density, sky-view factor and building frontal area ratio are widely used to investigate the relationship between urban morphology and ventilation. Hence, these parameters are selected for the systematic evaluation of the urban ventilation potential (*Table 2*). The urban morphology indicators are calculated from building survey data and resampled to 50 m, 100 m, 200 m, 300 m and 500 m scales. The 300-meter scale is selected, as it does not lose too much detail and is not misleading.

Table 2. Comprehensive information on the selected indicators

Morphological indicators retrieved from building survey data		
BD	The total area of the building divided by the pixel area	[0,1]
BH	The area-averaged building height	[0, max]
BVD	A 3D indicator calculated as the building volume divided by the pixel area	[0, max]
SVF	The fraction of sky visible at a given point	[0,1]
FAR	Total front area divided by the pixel area	[0, max]

3.2 Land Surface Temperature Time-Series Clustering

3.2.1 The LST Retrieval

In this paper, Landsat 8 OLI data was used to carry out the inversion of the urban surface temperature through the classic radiative transfer equation (RTE). The thermal infrared radiance value L_λ received by the satellite sensor is composed of three parts: the atmospheric upward radiance L, the actual radiance of the ground reaching the energy of the satellite sensor after passing through the atmosphere (the atmosphere radiates downward and reflects energy as it reaches the ground) and the thermal infrared radiation luminance value received by the satellite sensor L_λ. The RTE is then:

$$L_\lambda = [\varepsilon B(T_S) + (1-\varepsilon)L\downarrow]\tau + L\uparrow, \tag{3.1}$$

Where ε is the surface-specific emissivity, T_S is the actual surface temperature (K), $B(T_S)$ is the black-body thermal radiance and τ is the permeability of the atmosphere in the thermal infrared band (Sobrino, Jiménez-Muñoz, & Paolini, 2004).

3.2.2 The Spatial-Temporal Pattern

The commonly used methods for time series clustering include *k*-means, *k*-cdba, *k*-shape, and so forth, among which the *k*-means method is the most robust for experimental comparisons. In the dataset for the land surface temperatures and times, the study area is divided into multiple geographical clusters with a uniform distribution over time via the *k*-means method. Using the *k*-means algorithm for unsupervised classification as opposed to supervised classification provides the following advantages: (1) the classification center is selected solely from the inherent data characteristics, needing neither human intervention nor any defaults; (2) it classifies all pixels according to Euclidean distance in high-dimensional space so that the classification results better retain the variance in the data naturally, resulting in the largest possible differences between classes and the smallest possible differences within classes (Wang, J. & Ouyang, 2017); furthermore, for the time-series clustering, the time distance is taken into account.

Specifically, for any pixel *n* in the range of the study area, there is a vector *p* with *d* indicators. For the experiment in this paper, *d*=7. For all pixels, there are vector families (p_1, p_2..., p_n). The purpose of *k*-means is to divide all *n* pixels into *K* clusters in this 7-dimensional space, so as to minimize the Euclidean distance to each pixel in the high-dimensional space. The result of selecting the appropriate *K* value can be expressed as:

$$\arg\min \sum_{i=1}^{k} \sum \|p - \mu_i\|^2, \tag{3.2}$$

where *k* is the number of classes selected in the optimal clustering, μ_i is the clustering centre of class *i*, that is, the average vector of dimension *d* in this class *i*.

3.3 Identification of the Distribution and Diffusion Dynamic of Urban Air Pollution

3.3.1 Hybrid Single-Particle Lagrangian Integrated Trajectory (HYSPLIT) Model

The mixed single-particle Lagrangian composite trajectory model (HYSPLIT) (Draxler & Hess, 1998) developed by NOAA's Air Resources Laboratory (ARL) is a complete system for calculating simple air-parcel tracks as well as complex transport, dispersion, chemical conversion and deposition simulations. HYSPLIT remains one of the most widely used atmospheric transport and diffusion models in the field of atmospheric science. One of the most common applications of the model is reverse trajectory analyses to determine the origin of air masses and establish source-receptor relationships (Fleming, Monks, & Manning, 2012). It is also used in various simulations of atmospheric transport, dispersion and deposition of pollutants and hazardous substances.

3.3.2 Geographically Weighted Regression (GWR)

Unlike a conventional (global) regression model, GWR is able to model spatial variations in the relationship between dependent and independent variables (Liu, Zhan, Gao, et al., 2019). A GWR model takes the following form:

$$y_0 = \beta_0(u_i, v_i) + \sum_{k=1}^{p} \beta_k(u_i, v_i)\, x_{ik} + \varepsilon_i, \tag{3.3}$$

where y_0, x_{ik}, and ε_i are the dependent variables, the k^{th} independent variable (subscripted as k), and the random error at point i (subscripted as i), respectively. The location of a given point i is denoted by the coordinates (u_i, v_i). The coefficients $\beta_k(u_i, v_i)$ are the location-varying weights, and $\beta_0(u_i, v_i)$ is the geographically-varying intercept. Thus, the GWR extends the global regression model by adding the geographical location parameter to generate the local coefficients accounting for spatial non-stationarity. The estimates of $\beta_0(u_i, v_i)$ and $\beta_k(u_i, v_i)$ are based on the unbiased estimation of a set of observations, in which the weight matrix is used to weight the observations differently The variation in $\beta_k(u_i, v_i)$ at different locations makes the GWR different from the Ordinary Least Squares (OLS) method (Zhao et al., 2018).

4. RESULTS AND DISCUSSION

4.1 Urban Ventilation Potential

As shown in *Figure 3*, the dominant summer wind direction in Xiangyang is southeast to northwest, with the main wind channels distributed along the Han River and Jiao Liu line railway. However, due to the barrier imposed by the mountains, the wind direction changes at the local scale. The wind speed is higher on Wolong Avenue, which is located between Xian Mountain and the Lumen Mountains, due to the narrow pass there. At the same time, as the Han River flows from southeast to south in Yuliangzhou, there are inland sea-

land breezes along the Han River that flow from the river to the city. Overall, the winds in downtown Xiangyang are milder, with fewer windy days and gales. In addition, the built-up area has an impact on wind speed, with secondary wind channels within the built-up area mainly along the main road. In the downtown areas, the Fancheng and Xiangcheng Districts have predominately south winds, whereas the Xiangzhou District has predominately southeast winds (*Figure 3a*).

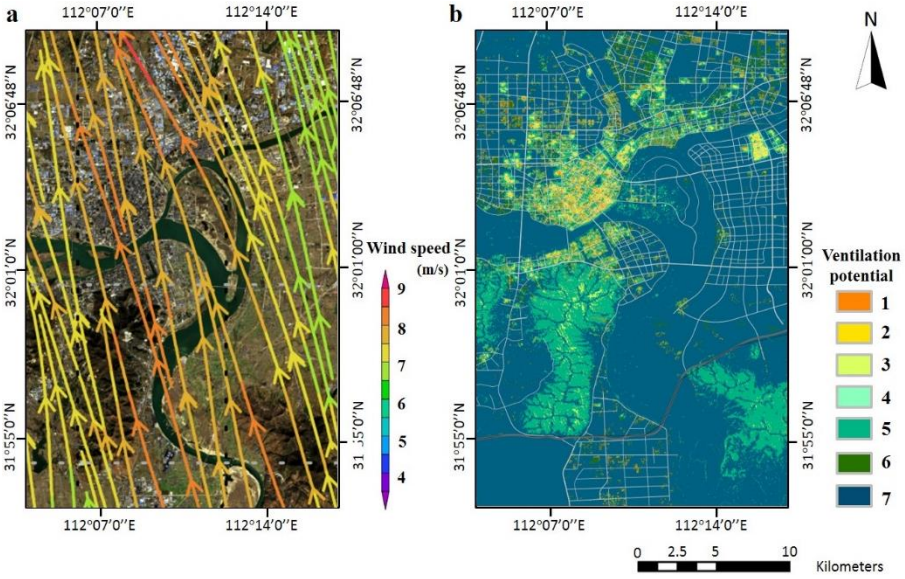

Figure 3. Assessments for: (a) wind distribution; (b) ventilation potential

The building morphological indicators are used to calculate the local ventilation potential, and possible ventilation corridors are tapped. The parameters used in the construction of the comprehensive ventilation potential evaluation indicator system include building density, building volume density and the downtown's windward surface density. As shown in *Figure 3b*, the ventilation potential rises from low to high, with 1 indicating that ventilation is most affected, and 7 indicating that it is not affected. The results show that the ventilation potential is lower in urban centers due to the high intensity of construction and that the hills also have an impact on urban ventilation, although not as strong an impact as in the built-up areas. However, in some areas, local wind conditions can also be fine, and these spaces are usually water bodies, open spaces, green spaces and wide roads. In addition, once these spaces are strung together, there is a good ventilation corridor within the city.

4.2 Urban Thermal Environment

As can be seen from *Figure 4*, the spatial pattern of the urban heat island effect from 2013 to 2016 shows obvious evolutionary changes. However, due to the influence of atmospheric hydrological conditions and cloud cover, the absolute mean temperature of the surface temperature time series images that can be adopted have statistically significant fluctuations and time heterogeneities, e.g., 2013 (37.23 ℃), 2014 (39.94 ℃), 2015 (33.96 ℃) and 2016 (30.44 ℃), and do not form a continuous time series. The trend in the urban heat island effect cannot be directly reflected by fluctuations in average air temperatures and average surface temperatures. Similarly, the UHI (urban heat island) images do not intuitively recognize spatio-temporal patterns. The

strongest heat island effects are concentrated in the northern industrial parks and central urban areas. Among them, the heat island intensity in the northern industrial park shows a continuous upward trend, and the heat island effect in Dongjin District is also increasing in parallel with the intensity of construction. It is worth noting that the heat island effect in Yuliangzhou, which was originally an ecological reserve, has increased in intensity in recent years due to the growth of tourism. The above conclusions are based on intuitive visual decoding with questionable reliability, some of which can be solved by the application of time-series clustering.

Time-series clustering can identify the rules and patterns in changes among clusters, so it can solve incomparability problems involving similar images in a long time series that are caused, to a certain extent, by time heterogeneity. The clustering results for surface temperature in Xiangyang show the robustness of the temporal clustering method, which is in line with intuitive perceptions and expectations. Cluster 1 represents an extremely strong heat island area from beginning to end; it is mainly an industrial area and a high-intensity construction area. Cluster 2 also represents a built-up area and heat island concentration area, but the intensity for this cluster is lower than that for Cluster 7, partly due to the expansion area of the heat island. Cluster 3 is mostly impermeable to water and also a potential heat island area. Cluster 4 is also a potential heat island area. The overall heat island intensity for Cluster 4 is lower than that of Cluster 3, but its heat island intensity has increased significantly in the past four years. Cluster 5 is the main water area, which can be considered to be the Han river. Both Cluster 6 and Cluster 7 can be considered to be vegetation-covered areas. Among them, Cluster 7 can be considered to be a cold island, as it is mainly composed of mountains and concentrated green land and wetlands (*Figure 5*).

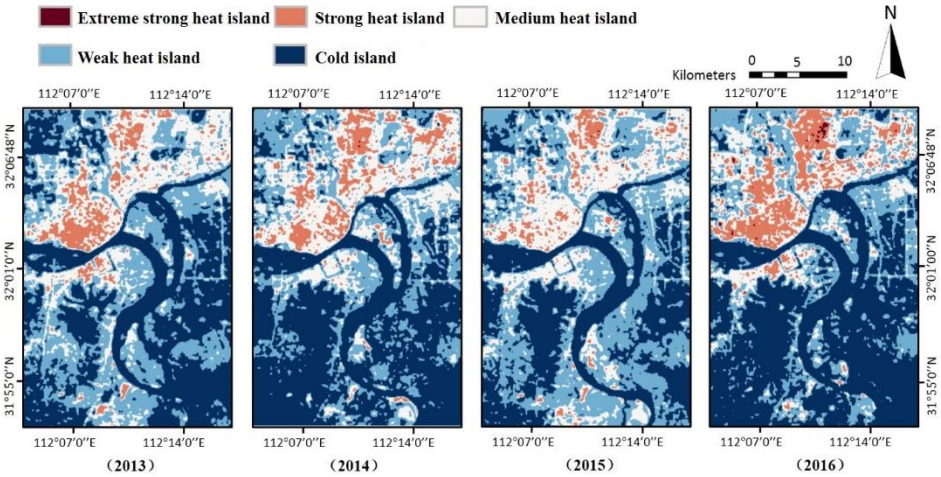

Figure 4. The spatial distributions of the land surface temperatures (LSTs)

Major urban heat islands are concentrated in the downtown areas, including Xiangcheng District, Fancheng District, Xiangzhou District and the industrial park to the north, and there are also small heat islands in Yujiahu to the south. From 2013 to 2016, due to the urban expansion, the heat island patches in the northern industrial park, Dongjin District and the Yujiahu industrial park have been expanding continuously, and the downtown Xiangzhou District has been transformed from the original sporadic heat island to a concentrated heat island. Meanwhile, the heat island intensity of the northern industrial park is at the highest in the entire city. The heat island patches around Xiangyang airport are expanding due to increased

impermeability. After 2013, the heat island effect in Yuliangzhou, which was not originally a region with a severe heat island effect, increased gradually.

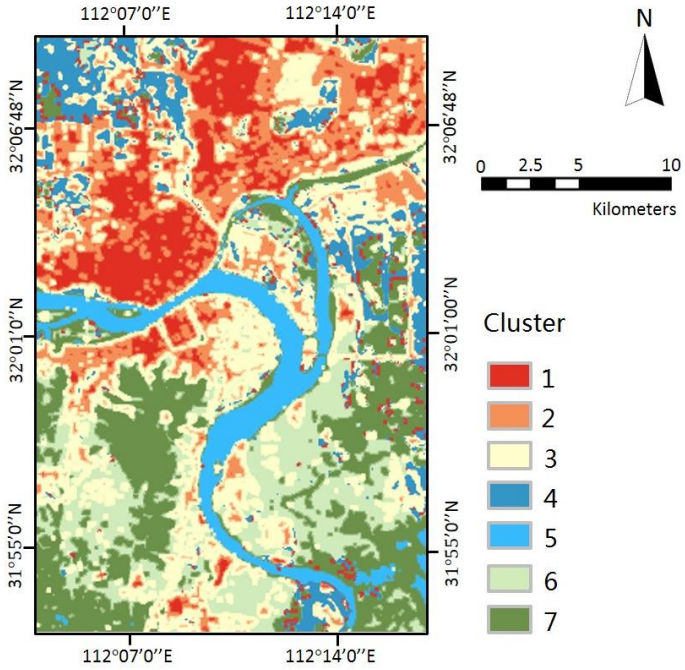

Figure 5. Time-series clustering results

4.3 The Sources and Diffusion of Air Pollution

4.3.1 The HYSPLIT Results

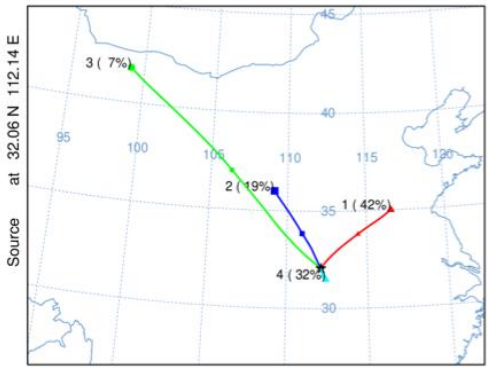

Figure 6. The HYSPLIT results

In this study, pollution within 300 km from Xiangyang's downtown is defined as being part of the local air masses for Xiangyang and is considered to have a short-range trajectory; within 600 km, the pollution has a medium-range trajectory; and beyond 600 km, the pollution has a long-range trajectory. In winter, the number of short-range pollution trajectories in Xiangyang accounted for 37.6% of the total trajectories, 28.2% of the medium-range trajectories and 34.2% of the long-range trajectories, indicating that the atmospheric diffusion conditions in Xiangyang are not ideal in winter and that pollution tends to gather during this period, resulting in fog. In winter, sand and dust from the southern Xinjiang basin, central and western Inner Mongolia, northern Ningxia and other places southward as well as air pollution from northern China, the Huang Huai Valley and the Jiang Huai fan-

shaped plain area also flood into the Nanyang-Xiangyang basin, thus superimposing on local pollutants and causing serious air pollution. The main sources of pollution are the North China region, the fan-shaped plains of the Yellow and Huaihe River basins and the Jiangsu-Huaihe River basin (42%), the Guanzhong plain and the loess plateau in northern Shaanxi (19%), while the smallest sources are the southern border basin, central and western Inner Mongolia and northern Ningxia (7%) (*Figure 6*).

4.3.2 The Result of GWR

In this study, the air pollution site data on February 9, 2018 was selected for regression analysis, and the air pollution distribution image, as obtained through interpolation using the kriging method, was used as the dependent variable. Morphological indicators such as building density (BD), average building height (BH), building volume density (BVD) and land cover indicators, such as NDBI (Normalized Building Index), NDVI (Normalized Vegetation Index), proportion of water body, proportion of industrial land, as well as the population density distributions of social and economic indicators, were selected as independent variables for geographically weighted regression, all of which were resampled to 500 m. According to the results obtained from the analysis (*Figure 7*), the GWR series models are superior to OLS models in terms of goodness-of-fit, although the R^2 is limited to 0.46. The distribution of local R^2 values is shown in the figure above, which indicates that the south is in better condition than the north. At the same time, the selected indicators provide a weak interpretation of the air pollution distribution, so more indicators need to be added to the regression to improve the goodness-of-fit. On the one hand, the additions may be necessary because the optimal research scale of air pollution is actually greater than 500 meters; on the other hand, the detection results of stations where air pollution distribution is greatly affected by wind direction and wind speed may not truly reflect the sources of air pollution. Meanwhile, as mentioned above, endogenous air pollution only accounts for part of the total air pollution, and most exogenous air pollution cannot be explored and identified via the GWR model.

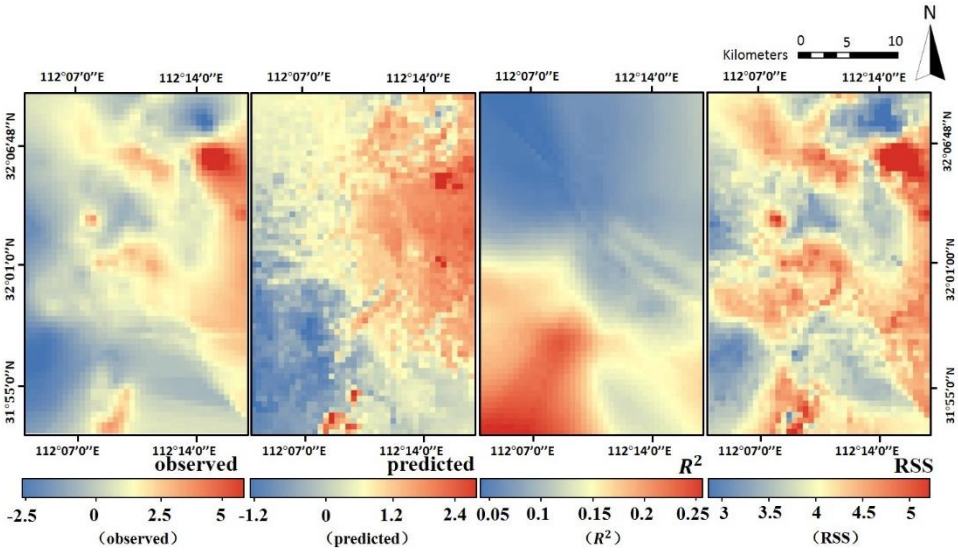

Figure 7. The GWR results

The high-level air pollution concentration areas are distributed within the Yujiahu industrial park in the south and the Shenzhen industrial park in the

northeast. In future studies, the influence of industrial formats on air pollution distribution can be further discussed. The coefficients and slopes of various indicators for the GWR regression results are shown in *Figure 8*. Meanwhile, representative indicators, such as the industrial land use ratio, water body ratio, NDBI and NDVI are selected for detailed analyses in this paper. Numerically, at the internal scale of the city, the industrial land contributes most to the haze, while the urban green space has a clear role in settling the haze. Building indicators contribute to the generation of haze, but the relationship is not significant enough, and the mechanism of action is not clear. Water bodies have a weaker impact on haze than greenfield vegetation, and this impact is dependent on natural river patterns. Spatially, because it is located on the main ventilation corridor, the development and construction of the Panggong area has had a great impact on air pollution diffusion. Water bodies and green spaces play obvious roles in alleviating air pollution, while the Xian and Lumen mountains along the Hanjiang river play an obvious role in reducing air pollution. In addition, dust from construction sites/bare soil contributes significantly to the air pollution.

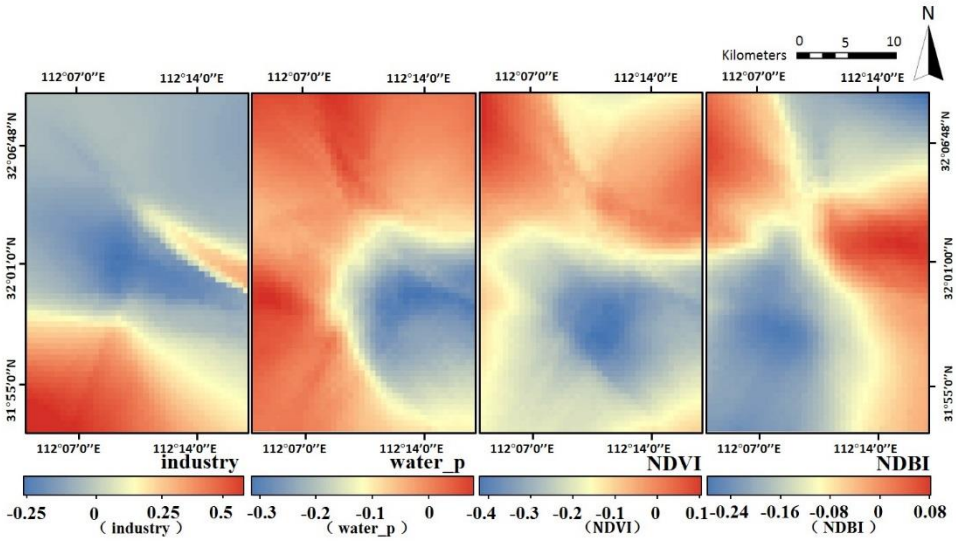

Figure 8. The spatial distributions of the indicators

4.4 Ventilation Corridor Planning Proposal

In this study, the influence of landscape composition and urban morphology on urban ventilation, the urban heat island effect and the urban pollution island effect, as well as the spatial heterogeneity of the strength of the influences, were discussed using various methods. More detailed information can be obtained through a study which considers time and space non-stationarity. A discussion of the results, application and limitations of this study are presented below.

4.4.1 The Influence of the Local Landscape and its Spatial Heterogeneity

The climatic response to this urban landscape had great spatial heterogeneity; therefore, it is crucial for climate modelling to take such spatial heterogeneity effects into consideration. Built-up areas make large contributions to the urban heat island effect, and this effect becomes more and more intense with the expansion of cities, while the contribution of land use

is significantly different. Low-rise, high-density, built-up areas are urban heat island concentration areas, among which residential and industrial areas are hot spots for pollution. Industrial zones contribute greatly to the urban heat island effect and urban air pollution, and different industrial formats have different contributions to the two. Green land and water have strong mitigation effects on the urban heat island effect and urban air pollution; meanwhile, the cooling and evacuation effects of the surrounding areas are also obvious.

4.4.2 Integration with Planning Practice

According to the above results, the operational areas, compensation areas and ventilation corridors are defined and corresponding planning measures are set up.

Figure 9. Urban ventilation corridor planning in Xiangyang

The operational areas are mainly concentrated in the commercial and residential areas as well as in the industrial areas to the south and north of the main urban area. In particular, the central business district contains most of the commercial areas; the low-rise, high-density residential area surrounds it; and the industrial areas include an aerospace industrial park to the northwest, the Shenzhen industrial park to the northeast and the Yujiahu industrial park to the south. The compensation areas are the water bodies and green spaces.

Several major lakes downtown and several large surrounding reservoirs constitute the main water compensation areas. Xian mountain, Lumen mountain and other forest parks are the first-level green space compensation areas, and the larger urban parks constitute the second-level green space compensation areas. Ventilation corridors are also divided into three classes: the first class consists of the main water bodies, the second class is made up of the major avenues, and the tertiary class consists of the sub-arterial highways (*Figure 9*).

For major urban built-up downtown areas, the overall idea of planning control is to reduce the intensity of development, enrich the green infrastructure and emphasize mixed land use. To be specific, low-rise, high-density areas can be converted into high-rise, low-density areas when the development intensity needs to be reduced; however, the plot ratio must be maintained at a level that ensures that urban functions are preserved. At the same time, replacing swathes of high-rises with high-rise points and increasing the water and green areas is also a solution. Furthermore, for the industrial zones, in addition to increasing the green spaces and green isolation belts for these zones, their locations should be carefully selected to avoid situating them in the city's upper air outlet. In addition, the industrial processes should be improved to reduce air pollution. For the water bodies and urban green infrastructures in the compensation areas, in addition to the strict control of the water bodies themselves to ensure that there is no further deterioration, high-density construction should also be reduced within a certain range of these buffer zones. Ventilation corridor controls should include the corridor width, greening ratio and building heights and densities.

4.5 Limitations

There are several limitations worthy of further discussion. Firstly, the current zoning is too rough to provide more detailed information. The LCZ method should be explored with regards to its applicability and feasibility in further studies. Secondly, due to the differences in action scales and influence factors between urban heat and urban pollution islands, any unified zoning attempt would lead to misleading results and make it difficult to solve these issues. Urban zoning for dealing with different urban climate problems should be done separately, then compared, so the interactions between these methods may be discussed further. Thirdly, the time-series clustering method can be used to obtain both temporal and spatial characteristics, but the existing planning measures are usually only for a single temporal aspect, and it is difficult to respond effectively to changes occurring over time. Therefore, the gap between time-series cluster analysis and the planning response should be closed. Finally, for air pollution, the results obtained via the kriging method do not correspond exactly to the real situation, which may lead to local overestimations or underestimations. A more appropriate method should be found to improve the accuracy of air pollution estimates.

5. CONCLUSIONS

In this study, a series of state-of-the-art geospatial techniques, including WRF, time-series clustering, HYSPLIT and GWR, have been introduced to investigate the spatial-temporal characteristics of, and factors affecting, urban ventilation, urban heat islands and urban pollution islands. According to the

spatial heterogeneity of the results, different planning zones are created and different planning measures are proposed to meet the sustainable development goals. The main findings are as follows: (1) the appropriate operational scales for examining urban ventilation, urban heat islands and air pollution are not necessarily the same, with the scales for ventilation and air pollution being relatively large and more suitable for analysis at the regional scale; (2) the urban morphology has a great deal of influence on the near-surface ventilation potential, but the spatial heterogeneity of its influence on air pollution diffusion is not strong; (3) both exogenous pollution and endogenous pollution make obvious contributions to urban air pollution; (4) topography plays an important role in pollution diffusion, and the closure of a basin allows air pollution to collect; (5) urban function has a significant impact on urban climate, which needs to be discussed further, especially in term of concentrated residential and industrial districts. Generally, it is of great significance to put forward planning suggestions from the perspectives of urban form, urban land cover and urban landscape composition to alleviate urban climate problems.

ACKNOWLEDGEMENT

This research is supported by the National Natural Science Foundation (No. 51878515, 51378399, 41331175).

REFERENCES

Chen, L., & Dirmeyer, P. A. (2019). "Differing Responses of the Diurnal Cycle of Land Surface and Air Temperatures to Deforestation". *Journal of Climate*, *32*(20), 7067-7079. doi: https://doi.org/10.1175/JCLI-D-19-0002.1.

Chen, L., Zhang, M., Zhu, J., Wang, Y., & Skorokhod, A. (2018). "Modeling Impacts of Urbanization and Urban Heat Island Mitigation on Boundary Layer Meteorology and Air Quality in Beijing under Different Weather Conditions". *Journal of Geophysical Research: Atmospheres*, *123*(8), 4323-4344. doi: https://doi.org/10.1002/2017JD027501.

Dienst, M., Lindén, J., & Esper, J. (2018). "Determination of the Urban Heat Island Intensity in Villages and Its Connection to Land Cover in Three European Climate Zones". *Climate Research*, *76*(1), 1-15. doi: https://doi.org/10.3354/cr01522.

Dimitriou, K., & Kassomenos, P. (2014). "Indicators Reflecting Local and Transboundary Sources of Pm2.5 and Pmcoarse in Rome – Impacts in Air Quality". *Atmospheric Environment*, *96*, 154-162. doi: https://doi.org/10.1016/j.atmosenv.2014.07.029.

Draxler, R. R., & Hess, G. (1998). "An Overview of the Hysplit_4 Modelling System for Trajectories". *Australian meteorological magazine*, *47*(4), 295-308.

Fleming, Z. L., Monks, P. S., & Manning, A. J. (2012). "Review: Untangling the Influence of Air-Mass History in Interpreting Observed Atmospheric Composition". *Atmospheric Research*, *104-105*, 1-39. doi: https://doi.org/10.1016/j.atmosres.2011.09.009.

Fu, P., & Weng, Q. (2016). "A Time Series Analysis of Urbanization Induced Land Use and Land Cover Change and Its Impact on Land Surface Temperature with Landsat Imagery". *Remote sensing of Environment*, *175*, 205-214. doi: https://doi.org/10.1016/j.rse.2015.12.040.

Gholizadeh, A., Neshat, A. A., Conti, G. O., Ghaffari, H. R., Aval, H. E., Almodarresi, S. A., . . . Miri, M. (2019). "Pm2.5 Concentration Modeling and Mapping in the Urban Areas". *Modeling Earth Systems and Environment*, *5*(3), 897-906. doi: https://doi.org/10.1007/s40808-019-00576-0.

Gsella, A., de Meij, A., Kerschbaumer, A., Reimer, E., Thunis, P., & Cuvelier, C. (2014). "Evaluation of Mm5, Wrf and Tramper Meteorology over the Complex Terrain of the Po Valley, Italy". *Atmospheric Environment*, *89*, 797-806. doi: https://doi.org/10.1016/j.atmosenv.2014.03.019.

He, B.-J., Ding, L., & Prasad, D. (2019). "Enhancing Urban Ventilation Performance through the Development of Precinct Ventilation Zones: A Case Study Based on the Greater Sydney, Australia". *Sustainable Cities and Society*, *47*, 101472. doi: https://doi.org/10.1016/j.scs.2019.101472.

Javanroodi, K., Mahdavinejad, M., & Nik, V. M. (2018). "Impacts of Urban Morphology on Reducing Cooling Load and Increasing Ventilation Potential in Hot-Arid Climate". *Applied energy*, *231*, 714-746. doi: https://doi.org/10.1016/j.apenergy.2018.09.116.

Jiménez, P. A., González-Rouco, J. F., García-Bustamante, E., Navarro, J., Montávez, J. P., de Arellano, J. V.-G., . . . Muñoz-Roldan, A. (2010). "Surface Wind Regionalization over Complex Terrain: Evaluation and Analysis of a High-Resolution Wrf Simulation". *Journal of Applied Meteorology and Climatology*, *49*(2), 268-287. doi: https://doi.org/10.1175/2009JAMC2175.1.

Kadaverugu, R., Sharma, A., Matli, C., & Biniwale, R. (2019). "High Resolution Urban Air Quality Modeling by Coupling Cfd and Mesoscale Models: A Review". *Asia-Pacific Journal of Atmospheric Sciences*, *55*(4), 539-556. doi: https://doi.org/10.1007/s13143-019-00110-3.

Kuang, W., Dou, Y., Zhang, C., Chi, W., Liu, A., Liu, Y., . . . Liu, J. (2015). "Quantifying the Heat Flux Regulation of Metropolitan Land Use/Land Cover Components by Coupling Remote Sensing Modeling with in Situ Measurement". *Journal of Geophysical Research: Atmospheres*, *120*(1), 113-130. doi: https://doi.org/10.1002/2014JD022249.

Liu, H., Zhan, Q., Gao, S., & Yang, C. (2019). "Seasonal Variation of the Spatially Non-Stationary Association between Land Surface Temperature and Urban Landscape". *Remote Sensing*, *11*(9), 1016. doi: https://doi.org/10.3390/rs11091016.

Liu, H., Zhan, Q., Yang, C., & Wang, J. (2018). "Characterizing the Spatio-Temporal Pattern of Land Surface Temperature through Time Series Clustering: Based on the Latent Pattern and Morphology". *Remote Sensing*, *10*(4), 654. doi: https://doi.org/10.3390/rs10040654.

Liu, H., Zhan, Q., Yang, C., & Wang, J. (2019). "The Multi-Timescale Temporal Patterns and Dynamics of Land Surface Temperature Using Ensemble Empirical Mode Decomposition". *Science of the Total Environment*, *652*, 243-255. doi: https://doi.org/10.1016/j.scitotenv.2018.10.252.

Oke, T. R., Mills, G., Christen, A., & Voogt, J. A. (2017). *Urban Climates.* Cambridge University Press. Retrieved from https://books.google.com/books?id=7h0xDwAAQBAJ.

Patz, J. A., Campbell-Lendrum, D., Holloway, T., & Foley, J. A. (2005). "Impact of Regional Climate Change on Human Health". *Nature*, *438*(7066), 310-317. doi: https://doi.org/10.1038/nature04188.

Peng, J., Jia, J., Liu, Y., Li, H., & Wu, J. (2018). "Seasonal Contrast of the Dominant Factors for Spatial Distribution of Land Surface Temperature in Urban Areas". *Remote sensing of Environment*, *215*, 255-267. doi: https://doi.org/10.1016/j.rse.2018.06.010.

Schindler, M., Caruso, G., & Picard, P. (2017). "Equilibrium and First-Best City with Endogenous Exposure to Local Air Pollution from Traffic". *Regional Science and Urban Economics*, *62*, 12-23. doi: https://doi.org/10.1016/j.regsciurbeco.2016.10.006.

Sharma, S., Chatani, S., Mahtta, R., Goel, A., & Kumar, A. (2016). "Sensitivity Analysis of Ground Level Ozone in India Using Wrf-Cmaq Models". *Atmospheric Environment*, *131*, 29-40. doi: https://doi.org/10.1016/j.atmosenv.2016.01.036.

Shi, Y., Ren, C., Lau, K. K.-L., & Ng, E. (2019). "Investigating the Influence of Urban Land Use and Landscape Pattern on Pm2.5 Spatial Variation Using Mobile Monitoring and Wudapt". *Landscape and urban planning*, *189*, 15-26. doi: https://doi.org/10.1016/j.landurbplan.2019.04.004.

Sobrino, J. A., Jiménez-Muñoz, J. C., & Paolini, L. (2004). "Land Surface Temperature Retrieval from Landsat Tm 5". *Remote sensing of Environment*, *90*(4), 434-440. doi: https://doi.org/10.1016/j.rse.2004.02.003.

Song, J., Du, S., Feng, X., & Guo, L. (2014). "The Relationships between Landscape Compositions and Land Surface Temperature: Quantifying Their Resolution Sensitivity with Spatial Regression Models". *Landscape and urban planning*, *123*, 145-157. doi: https://doi.org/10.1016/j.landurbplan.2013.11.014.

Stewart, I. D., & Oke, T. R. (2012). "Local Climate Zones for Urban Temperature Studies". *Bulletin of the American Meteorological Society*, *93*(12), 1879-1900. doi: https://doi.org/10.1175/BAMS-D-11-00019.1.

Stone, B. (2009). "Land Use as Climate Change Mitigation". *Environmental Science & Technology*, *43*(24), 9052-9056. doi: https://doi.org/10.1021/es902150g.

Sun, R., Lü, Y., Yang, X., & Chen, L. (2019). "Understanding the Variability of Urban Heat Islands from Local Background Climate and Urbanization". *Journal of Cleaner Production*, *208*, 743-752. doi: https://doi.org/10.1016/j.jclepro.2018.10.178.

Tsichritzis, L., & Nikolopoulou, M. (2019). "The Effect of Building Height and Façade Area Ratio on Pedestrian Wind Comfort of London". *Journal of wind engineering and industrial aerodynamics*, *191*, 63-75. doi: https://doi.org/10.1016/j.jweia.2019.05.021.

Wang, C., Li, Y., Myint, S. W., Zhao, Q., & Wentz, E. A. (2019). "Impacts of Spatial Clustering of Urban Land Cover on Land Surface Temperature across Köppen Climate Zones in the Contiguous United States". *Landscape and urban planning*, *192*, 103668. doi: https://doi.org/10.1016/j.landurbplan.2019.103668.

Wang, J., & Ouyang, W. (2017). "Attenuating the Surface Urban Heat Island within the Local Thermal Zones through Land Surface Modification". *Journal of environmental management*, *187*, 239-252. doi: https://doi.org/10.1016/j.jenvman.2016.11.059.

Wang, J., Zhan, Q., & Guo, H. (2016). "The Morphology, Dynamics and Potential Hotspots of Land Surface Temperature at a Local Scale in Urban Areas". *Remote Sensing*, *8*(1), 18. doi: https://doi.org/10.3390/rs8010018.

Wang, Z.-b., & Fang, C.-l. (2016). "Spatial-Temporal Characteristics and Determinants of Pm2.5 in the Bohai Rim Urban Agglomeration". *Chemosphere*, *148*, 148-162. doi: https://doi.org/10.1016/j.chemosphere.2015.12.118.

Xie, W., Deng, H., & Chong, Z. (2019). "The Spatial and Heterogeneity Impacts of Population Urbanization on Fine Particulate (Pm2.5) in the Yangtze River Economic Belt, China". *International journal of environmental research and public health*, *16*(6), 1058. doi: https://doi.org/10.3390/ijerph16061058.

Xie, Y., Wang, Y., Zhang, K., Dong, W., Lv, B., & Bai, Y. (2015). "Daily Estimation of Ground-Level Pm2.5 Concentrations over Beijing Using 3 Km Resolution Modis Aod". *Environmental Science & Technology*, *49*(20), 12280-12288. doi: https://doi.org/10.1021/acs.est.5b01413.

Xu, Y., Ren, C., Ma, P., Ho, J., Wang, W., Lau, K. K.-L., . . . Ng, E. (2017). "Urban Morphology Detection and Computation for Urban Climate Research". *Landscape and urban planning*, *167*, 212-224. doi: https://doi.org/10.1016/j.landurbplan.2017.06.018.

Yang, B., Zhang, Y., & Qian, Y. (2012). "Simulation of Urban Climate with High-Resolution Wrf Model: A Case Study in Nanjing, China". *Asia-Pacific Journal of Atmospheric Sciences*, *48*(3), 227-241. doi: https://doi.org/10.1007/s13143-012-0023-5.

Yang, C., Zhan, Q., Gao, S., & Liu, H. (2019). "How Do the Multi-Temporal Centroid Trajectories of Urban Heat Island Correspond to Impervious Surface Changes: A Case Study in Wuhan, China". *International journal of environmental research and public health*, *16*(20), 3865. doi: https://doi.org/10.3390/ijerph16203865.

Yang, C., Zhan, Q., Zhang, J., Liu, H., & Fan, Z. (2018). "Quantifying the Relationship between Natural and Socioeconomic Factors and with Fine Particulate Matter (Pm2.5) Pollution by Integrating Remote Sensing and Geospatial Big Data". *Int. Arch. Photogramm. Remote Sens. Spatial Inf. Sci.*, *XLII-3/W5*, 77-82. doi: https://doi.org/10.5194/isprs-archives-XLII-3-W5-77-2018.

Yin, C., Yuan, M., Lu, Y., Huang, Y., & Liu, Y. (2018). "Effects of Urban Form on the Urban Heat Island Effect Based on Spatial Regression Model". *Science of the Total Environment*, *634*, 696-704. doi: https://doi.org/10.1016/j.scitotenv.2018.03.350.

Yu, X., Guo, X., & Wu, Z. (2014). "Land Surface Temperature Retrieval from Landsat 8 Tirs—Comparison between Radiative Transfer Equation-Based Method, Split Window Algorithm and Single Channel Method". *Remote Sensing*, *6*(10), 9829-9852. doi: https://doi.org/10.3390/rs6109829.

Zhao, C., Jensen, J., Weng, Q., & Weaver, R. (2018). "A Geographically Weighted Regression Analysis of the Underlying Factors Related to the Surface Urban Heat Island Phenomenon". *Remote Sensing*, *10*(9), 1428. doi: https://doi.org/10.3390/rs10091428.

Zhou, X., & Chen, H. (2018). "Impact of Urbanization-Related Land Use Land Cover Changes and Urban Morphology Changes on the Urban Heat Island Phenomenon". *Science of the Total Environment*, *635*, 1467-1476. doi: https://doi.org/10.1016/j.scitotenv.2018.04.091.